Review Article
Published: 26 Jan, 2018

SF Journal of Material and Chemical Engineering

From Powder to Power: Ukrainian Way

Vasylyev OD[1]*, Brodnikovskyi YM[1], Brychevskyi MM[1], Polishko IO[1], Ivanchenko SE[2] and Vereshchak VG[3]

[1]Laboratory for Ceramic Fuel Cells, Frantcevych Institute for Problems of Materials Science, Ukraine

[2]Department of Physical Chemistry and Technology of Nanostructural Ceramics and Composites, Frantcevych Institute for Problems of Materials Science, Ukraine

[3]Laboratory for Chemistry and Technology of Powder Materials, Ukrainian State University of Chemical Technology, Ukraine

Abstract

The paper is a short surwey of the R&D activity of Laboratory for Ceramic Fuel Cells at Frantcevych Institute for Problems of Materials Science, Ukraine, on their way from cubic zirconia powder development to creation and elaboration of Ceramic (Solid Oxide) Fuel Cells. Such the research topics, which are important for the further development of Ceramic Fuel Cells, like 1Ce10ScSZ zirconia powders, formation of structure and strength of zirconia electrolytes, structure and properties of EB-PVD films, conductivity of bulk and film 1Ce10ScSZ electrolyte, catalitic activity of zirconia powders, reduction of nickel, redox of Ni – ZrO_2 composites, and structural optimization of CFC, are discussed. Comparative test of developed CFC and commercial one is completing the review.

Keywords: 1Ce10ScSZ zirconia powders; Zirconia electrolyte; Porous NiO–ZrO_2 composite; Ni reduction; Ceramic fuel cell; Solid oxide fuel cell; Zirconia EB-PVD film; Catalytic activity; Redox

Introduction

Historically, Fuel Cells have been innovated as chemical phenomenon and device based on liquid electrolytes – water solutions of acids. The first Fuel Cells are obvious to be realized with participation of materials, first, with help of platinum electrodes. Solid Oxide Fuel Cells can be implemented only as material objects because require the solid electrolyte able to withstand aggressive fuels and oxygen.

For more than a hundred years of their development, Solid Oxide Fuel Cells (SOFCs) have proved their high efficiency, reliability, and ability to diminish environmental pollution related to production of electricity and heat, internal combustion engines etc.

By its nature, SOFC is a layered metal-ceramic device that is traditionally produced by ceramic technologies, main of which are powders and their sintering. That is the reason why SOFC is named often as Ceramic Fuel Cell (CFC), and CFC success is resulted mainly from successes of chemical and ceramic technologies in production of powders and their consolidation. In such a way, it is possible to trace the way from powders to electric power that logically sounds very impressively. For the first time, we have heared the expression “From powder to power” from K. Föger at his unpublished conference presentation [1] with the attractive pictures of research activity in Australia where impressive CFC energy system Bluegen was developed by Ceramic Fuel Cell Ltd. to be based on both the knowledge “What is zirconia?” and “How must zirconia powders be produced and transformed into CFC?”. Now, according the “From powder to power” principle, not only powder transformation into some end-product, in our case – power, is considered, but competing products are compared also.

The goal of this paper is to give a short review of the R&D activity of Laboratory for Ceramic Fuel Cells that was formally founded in 2015 at Frantcevych Institute for Problems of Materials Science, Ukraine. The fuel cells have a special interest because they were practically banned till 2000 year for non-secret R&D not only in Ukraine but in all the former Soviet Union. Moreover, this activity concerns the development of Ukrainian zircon-sand deposit that is the third in the World after Australia and South Africa, and the largest in all the Northern hemisphere.

The SOFC activity in Ukraine is based on our former R&D activity on powders of yttria

OPEN ACCESS

***Correspondence:**
Vasylyev OD, Laboratory for Ceramic Fuel Cells, Department of Physics of Strength and Plasticity of Materials, Institute for Problems of Materials Science, Krzhizhanovsky Street, Ukraine.
Tel: *+380444240294*
E-mail: *oleksa.vasylyev@gmail.com*

Received Date: *23 Oct 2017*
Accepted Date: *15 Jan 2018*
Published Date: *26 Jan 2018*

Citation: *Vasylyev OD, Brodnikovskyi YM, Brychevskyi MM, Polishko IO, Ivanchenko SE, Vereshchak VG. From Powder to Power: Ukrainian Way. SF J Material Chem Eng. 2018; 1(1): 1001.*

ISSN 2643-8100

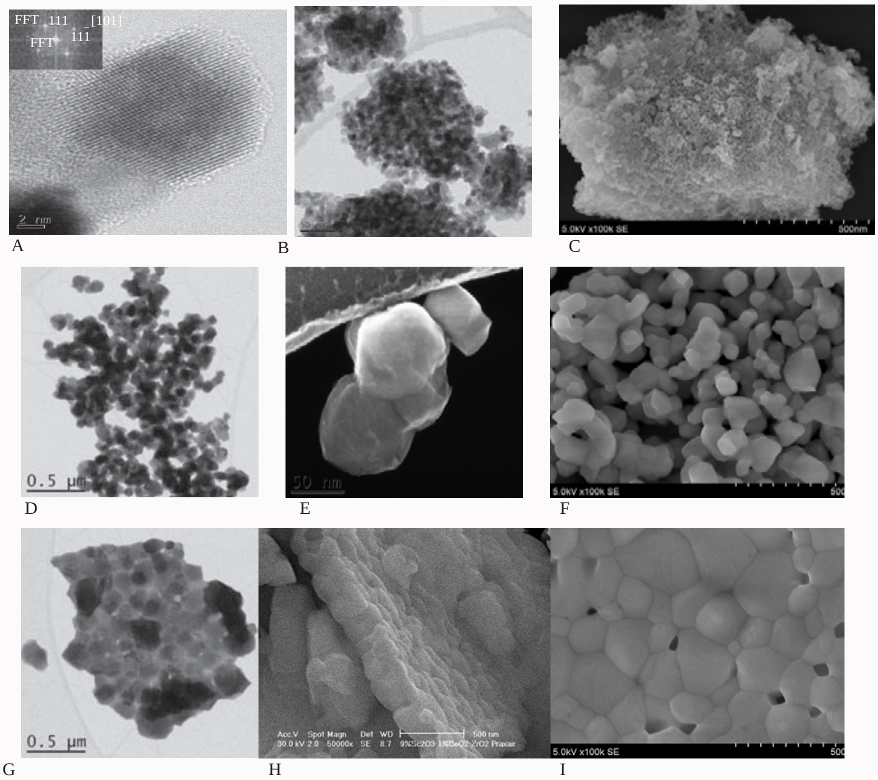

Figure 1: The high-resolution (A), conventional transmission (B,D,G) and scanning (E,F,H,I) electron microscopy images of three 10Sc1CeSZ powder Types (A,B,D-F) and their agglomerates (C,G-I). A-C – Type I, D-F – Type II, and G-I – Type III [4].

stabilized zirconia and zirconia structural ceramics, especially their mechanical behavior [2]. CFC research was initiated as voluntary activity, serious progress of which has been supported by research funds of NATO and European Union. This activity covers all topics of fuel cell creation beginning from development of special zirconia powders, their characterization and transformation into CFC parts and whole fuel cells, and CFC testing.

The paper consists of a few parts related to powders and their properties, their ceramics in bulk and EB-PVD film states and their properties, mechanical behavior and electrical conductivity. In short, formation of Ni – ZrO_2 anode electrode, its reduction as well as short-term tests of CFC is considered also. All the topics are directed on the structural optimization of CFC devices.

So, let's consider the topics mentioned.

Ce10ScSZ Zirconia Powders

Zirconia powders precipitating from water solutions are typical objects of chemical technologies though they must be considered also and as the physical objects because they nucleate, grow, and solidify, or condense, transforming into condensed solid matter that is a typical physical process.

1Ce10ScSZ (1-mol. % CeO_2 – 10-mol. % Sc_2O_3 – 89-mol. % ZrO_2) electrolyte ceramics are considered as the most promising electrolyte for CFC because they are able to ensure the higher (around one order of magnitude) ionic conductivity that yttria stabilized one.

Three types of formally the same chemical composition 10Sc1CeSZ zirconia powders were tested. They were made using different initial raw materials and synthesis conditions resulting in different morphology, impurities, and their distribution across the powders. The powders were subjected to comprehensive structural characterization with traditional analytical techniques and described in numerous literature [3,4].

The typification of powders has its origin in morphological and chemical features of their initial particles, morphological and mechanical properties of their agglomerates, ability to be sintered and mechanical behavior of their ceramics consolidated with uniaxial and cold isostatic pressing. The listed properties were obtained at comparative studies. The Type I powder (developed by V. Vereshchak and produced at Vilnohirsk Mining & Metallurgical Plant and Zirconia Ukraine Ltd. in Ukraine) was made by modified co-precipitation technique; the Type II powder delivered by Daiichi Kigenso Kagaku Kogyo (DKKK), Japan, was produced, as we might know, by the hydrothermal synthesis, and the Type III powder delivered by Praxair, USA, was made by spray-pyrolysis.

As to the structural and mechanical properties of these powders, here we remind only that the Type I powder is agglomerated in ~2.5µ semisoft-semirigid creatures of rod-like morphology consisting of 11±2 nm initial particles; the Type II is practically non-agglomerated and consist of soft 73±20 nm particles of an isotropic morphology, and the Type III is agglomerated in ~1.3µ rigid rapidly solidified ceramic husk-like creatures, which are, in fact, as thin plates of well-sintered ceramics hardly able to the further sintering. The electron microscopy pictures of all the powders are gathered in Figure 1.

We would like to remind also that the initial carriers of dopants, contaminants or impurities are surfaces of initial particles and their agglomerates. Surfaces of initial particles are enriched by impurities / dopants as result of particle solidification. Number of admixtures on surfaces of initial particles and their agglomerates may differ significantly. During sintering they are redistributing between grains and their boundaries forming grain boundary complexions, which are transforming in the courses at their heat treatment at sintering. As to features of chemical composition of samples determined with wet-techniques, the concentration of impurities in the bulk made of the Type I and the Type III powders is around 0.01-wt. %. The Type II is much purer; it contains only 0.001-wt. % of impurities. Regarding the nature of the contaminants, the Type I is contaminated mainly with SiO_2 (~0.05%) and Al_2O_3 (<0.025%) while in the Type III – mainly SiO_2 (~0.05%) and TiO_2 (<0.14%) are present. Additional minor contamination by K, Na, Ca, and Fe was also found in Types I and III powders. From the point of surface-bulk distribution obtained with secondary ion mass spectroscopy, in the Type II, the surface of particles is enriched with Sc and Al; in the Type III, Sc and Si are mostly present on the surface. In the Type I, the surface is depleted with Sc; while Sc and Si are mostly localized in the bulk of the particles.

The realization of high oxygen ionic conductivity of solid electrolytes based on zirconia to be ensured with scandia is facing at least two problems.

The first one is a comparatively old problem of high temperature structural instability of scandia stabilized zirconia (SSZ) that results from arising high resistance phases in it [5,6]. The problem is solving by additional doping of zirconia with ~1-mol. % of the second stabilizer like Ce, Al, Ti etc. But, the second doping decreases the conductivity for around one order of magnitude, the reasons of which are still unclear. Both, chemical composition of electrolyte and its structure are not optimized yet. The first problem is related to electrolyte material that is considered as a separately located substance, which is beyond the fuel cell, i.e., it has no direct contacts with electrode materials and is not loaded by high temperature gases, which are different at each side of electrolyte film.

The second problem is a comparatively "fresh" one, which became considered only recently. It is defined as chemical and structural instability of electrolyte arising in it in a course of both production of CFC and its long term high temperature operation. It is clear, that the first problem is a part of the second one, where the electrolyte material is not only influenced by temperature, but its comparatively thin layer gets in contact with other materials by high energy method and exposes to reducing and oxidizing gases through contacting gas permeable porous electrode materials for a long time.

The second problem is a degradation problem of film electrolyte essentially, which is placed in the structure of laminated composite and exposed to aggressive high temperature environments, which are different on its both sides. Moreover, the electrolyte film is nucleating and growing on supporting electrode material from vapor phase of electrolyte material excited by electrons.

This problem is not only unstudied yet. It is formulated only now.

It sets the tasks to study as follows: How does electrolyte condense from the vapor phase and grow on the porous heterogeneous substrate?

- What is happening with electrolyte film when cathode material exposes it?
- What is happening with a material of rather thin (<10 μm) electrolyte film, which is placed between two different materials of electrodes, anode and cathode, during a comparatively short time of production at temperature above 1000°C in air at conventional technological CFC route and vacuum, in the case of application of EB-PVD technique?
- What is happening with electrolyte film during long term (thousands of hours) operation at, e.g., 600 – 800°C being exposed by reducing or redox atmospheres (fuel) at one side (anode) and oxidizing atmosphere (air) at another side affected through permeable materials of corresponding electrodes?

We know already that the electrolyte film of ~20μm thickness being deposited by EB-PVD technique on NiO-ZrO_2 anode during a rather short (less than 30 min) interval time deposition process is enriched with nickel, concentration of which near the anode-electrolyte interface consists of around 2-wt. % and around 1-wt. % near free film surface [7-9]. We see that electrolyte film is not only structurally but also chemically heterogeneous, in which, e.g., Ni, as well as Y that is not shown here, a gradient distribution across the film thickness occurs. There are some data pointing out that Ni could stabilize cubic structure of zirconia acting similar traditionally used Ce etc. [10-12], and this phenomenon is proposed to be used for correlation of the electrolyte composition. The similar phenomena occur probably on a cathode side of the electrolyte also.

The analogous changes in solid phases take place in the anode. Moreover, this phenomenon is enhanced under the action of hydrogen [13-15].

As to cathode, there are still no reliable data on its influence on structure of the electrolyte film.

Considering zirconia-based electrolyte materials as polycrystalline, it is usually believed that silica is decreasing conductivity of zirconia due to its segregation along grain boundaries. The logic is simple: smaller grain size – larger specific grain boundary surface – purer boundary – higher conductivity. However, as to silica, we see, the Type II electrolyte is generically purer (more than one order of magnitude – 0.004-wt. % in it – against 0.05-wt. % in the Type I or the Type III ones). The similar situation is observed with alumina. Suppose that segregation of silica along grain boundaries has increased indeed due to grain growth during around 150 hours that results in significant conductivity decrease observed (see below Figure 9). After this term, the conductivity of the silica doped electrolyte becomes unchangeable vs. time and equal to the conductivity of the purer electrolyte that is the Type II one.

Thus, zirconia based electrolyte of technical purity, doped with silica and alumina, ensure the same level of conductivity similar to its purer analogue. In that time, there are some structural states of 10Sc1CeSZ electrolyte that ensure significantly higher conductivity. However, this high level of conductivity is suppressed by elements, which are mutually diffusing between electrolyte and electrodes that takes place at both production of CFC, especially when EB-PVD technique is used, and during its operation that is probably promoted by hydrogen.

The cases mentioned are saying that in order to keep the ionic conductivity high enough and stable or even increased at a long time of operation, chemical composition and structure of electrolyte film might be optimized or, saying by other words, be correlated by taking into account their changes during both CFC production, especially with high-energy EB-PVD technique, and its operation at real environments. The correlation of electrolyte consists in modification of some initial chemical composition, which could be changed

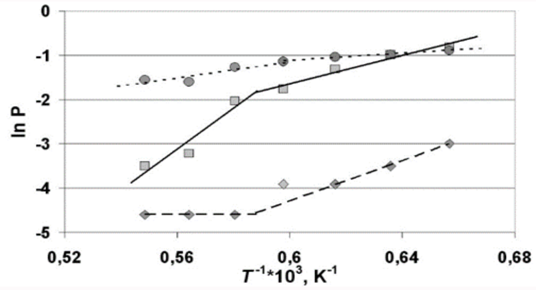

Figure 2: The Arrhenius's dependencies of porosity of ceramics made of 1Ce10ScSZ powders on sintering temperature. ● - Type I; ♦ - Type II, and ■ - Type III.

during the CFC production process and some (not very long) term of the CFC operation or its training, in order to produce finally some "ideal" composition that could ensure the best conductivity, which, additionally, might be even improved during operation instead of a traditional decrease with time.

The Formation of Structure and Strength of Bulk Zirconia Electrolyte

Structural parameters of sintered materials depend on sintering temperature. It was found that the joint consideration of the structure and mechanical behavior has proved to be fruitful for creation of the theory of formation of both the structure of solid electrolyte and the dependence of its strength on structural parameters and, in such a way, sintering temperature [16].

Considering the effect of sintering temperature on structure and mechanical behavior of zirconia electrolytes as well as processes of powder consolidation and structure refinement at sintering as thermally activated, the relations describing dependencies between strength and grains/subgrains, porosity, quality of boundaries and sintering temperatures, as well as imaginary activation energies determining densification or porosity, grain size growth, boundary states and strengthening / weakening at cleavage or intergranular fracture mechanisms were determined.

The dependence of porosity of ScSZ electrolyte *P* on sintering temperature T_s is shown in Figure 2. It is obvious that it might be approximated by the Arrhenius's exponents as

$$P = P_o \cdot exp\ (U_c / kT_s),$$

where U_c is the imaginary activation energy of densification, *k* – Boltzmann's constant.

It is seen that ability to densification is different in all the ceramics. Figure 2 shows clearly that the dependencies of porosity vs. sintering temperature are consisting of two parts: low and high temperature ones. The transition between them occurs in withinity of 1400–1450°C.

Each part (except of high temperature one in the Type II ceramics where the densification does not observe) has own the imaginary energy of activation, U_c, which are 0.35 and 0.78 eV in the Type I ceramics, 1.4 eV in the Type II ceramics sintered in its low-temperature stage, and 1.38 and 3.99 eV in the Type III ceramics, respectively (Table 1).

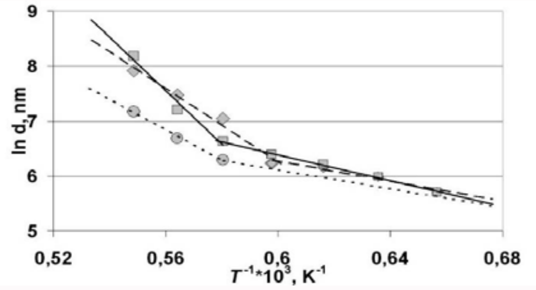

Figure 3: The Arrhenius's dependencies of average grain size of ceramics made of 1Ce10ScSZ powders on sintering temperature. ● - Type I; ♦ - Type II, and ■ - Type III.

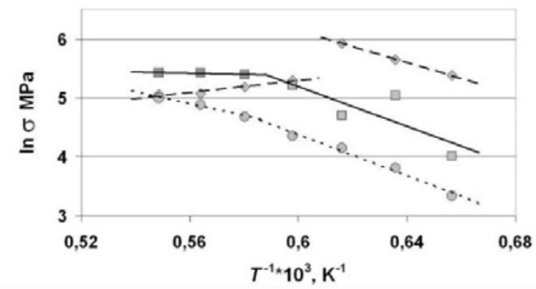

Figure 4: The Arrhenius's dependencies of room temperature biaxial strength of ceramics made of 1Ce10ScSZ powders on sintering temperature. ● - Type I; ♦- Type II, and ■ - Type III.

Table 1: The imaginary energies of activation of densification U_c, and grain growth U_{gg} of electrolyte ceramics sintered of three types of 1Ce10ScSC ceramics at temperatures below and higher their inflection points T_o.

Powder type	Imaginary activation energy, in average, *eV*			
	U_c		U_{gg}	
	Temperatures			
	$<T_o$	$>T_o$	$<T_o$	$>T_o$
I	0.35	0.78	-	2.65
II	1.4	~0	0.96	2.90
III	1.38	3.99	1.01	4.21

Except very different ability to densification, the ceramics have the different ability to grain growth also. The Arrhenius's dependencies of the average grain size on sintering temperature are shown in Figure 3. It is seen that the dependencies might be described by exponents also, however, here, we have to note that the interval of sintering temperatures studied comprises both sintering stages, namely, the stage of a final sintering and the stage of an intraagglomerate consolidation. The transition from low- to high-temperature part takes place near 1400 – 1450 °C that is well-coinciding with data on temperature dependence of grain growth in structural tetragonal zirconia ceramics Y-TZP where tetragonal structure of zirconia is stabilized by 3-mas. % of yttria [17]. It is noted there that the transition from slow to fast grain growth occurs in withinity of 1400°C. This transition results in a practically double growth of the activation energy from 2.80 to 5.46 eV.

It is obvious (Table 1) that the imaginary activation energy, U_{gg}, of grain size growth is radically different for different sintering stages and depends strongly on the powder type also. At the final sintering stage, the imaginary energies of activation are 2.65, 2.90 and 4.21 eV for the Type I, the Type II and the Type III electrolytes, respectively. For interagglomerate sintering, U_{gg} is similar in ceramics of II and III Types, 0.96 and 1.01 eV respectively.

Table 2: The imaginary activation energies of strengthening / weakening, U_s, of electrolyte ceramics sintered of three Types of 1Ce10ScSC ceramics at temperatures below and higher their inflection points T_o.

Powder type	Imaginary activation energy, U_s, in average, *eV*	
	Temperature	
	$<T_o$	$>T_o$
I	1.5	0.87
II	1.17	−0.43
III	1.46	0

As to the dependence of strength σ, and mechanical behavior in general, on sintering temperature might be defined as some function of structural constituents, first, porosity *P*, grain size *d* and some property *γ*, something like the surface energy, which describes quality of boundaries between structural constituents and depends on amount and ordering of admixtures along them.

In general, following [18], the strength σ in dependence on T_s might be described by a complex function as

$$\sigma(T_s) = f\{P(T_s), d(T_s), \gamma(T_s)\}.$$

The dependence of the biaxial strength measured at room temperature on sintering temperature is shown in Arrhenius coordinates in Figure 4. Unlike dependencies of porosity and grain size, they are not similar. Furthermore, the Type II curve has a discontinuity at the inflection point T_o in withinity 1375°C. The strength of each ceramic Type on sintering temperature may be described by two exponents as usual, but their imaginary activation energies are so different, magnitude and sign, that in the case of the Type II ceramics we should talk about weakening instead of strengthening.

Fracture mechanisms and strength of 1Ce10ScSZ electrolyte at room temperature are described in details in [3,16]. The imaginary energies of activation for strengthening / weakening, U_s, of three Types of 1Ce10ScSZ ceramics is given in Table 2.

Concerning the fractographical visualization of boundaries via their behavior under mechanical stresses at loading or their interaction with brittle cracks, it became possible to determine that they are brittle interpartial and intergranular (intergrain) fracture, and an alteration of cleavage plane and cracking at boundary crossing that could form so-called river patterns.

The detailed description of fractographical features of interaction of a brittle crack with structural elements of 1Ce10ScSZ ceramics in relation to electrical and chemical properties of their interfaces/boundaries is given in [19]. It was found that the heat (temperature-time) treatment via sintering and the powder typification are the suitable and convenient thermodynamical and chemical tools for the boundary engineering with "useful or non-useful" additives to control the boundary complexions and their transitions in sintered scandia stabilized zirconia electrolyte. Using this approach, the fullest variety of structural parameters such as porosity, sub grain and grain size growth and redistribution of additives across structural constituents and their boundaries, and altering their states have become available for the study. The joint analysis of data obtained with electron microscopy and related techniques, mechanical tests for strength, scanning electron fractography and impedance spectroscopy of structural constituents of electrical resistance is giving much more reliable information on the effect of boundaries and their complexions on properties of materials especially such as ceramic electrolytes where mechanical behavior is as important as their conductivity.

It was surprisingly found that the resistance of intergranular phases is near 30Ω·cm in all samples made of the Type I and Type III powders (they are of technical purity) sintered at all temperatures studied, and does not depend on the type and the amount of admixtures (either SiO_2 and Al_2O_3 in the Type I, either SiO_2 and TiO_2 in the Type III, either the third oxides (the total number of Si, Al, Ti, Fe oxides is ~0.01%) in the Type II at sintering temperatures below ~1375°C) and their distribution across the grains, grain size and general porosity.

Only in the Type II electrolyte, that is the purest, sintered at temperatures above ~ 1375°C, when this electrolyte does consist of recrystallized grains, the boundary resistance is abruptly decreasing from ~ 30 to 17 Ω.cm. Namely, in withinity of this temperature, the joint activation energy of numerous thermo activated processes of powder consolidation is changed, the grain bulk is purifying from the subgrain boundaries and non-numerous additives become distributed uniformly across grains as fractography evidences unambigously. The mechanical strength decreases here abruptly from 400 to 150 MPa as result of abrupt replacement of the effective strengthening structural element from subgrain (similar small grains) for much larger grains and, thereby, abrupt decrease of their number.

As to the grain bulk electrical resistance, it can be concluded that in Type I electrolyte, it decreases continuously from 14 to 6 Ω·cm with porosity decrease at 1300 – 1450°C and does not depend on structural evolution considering the cleavage fracture mechanism that may evidence continuous altering in the grain bulks and their boundaries with no any transitions, at least at temperatures in the interval studied. In Type II electrolyte, the grain body resistance cannot be detected indicating that the electrochemical properties of the grain bodies and their boundaries are the same, and the material looks like a single phase one. In Type III electrolyte, the resistance decreases from 20 to 5 Ω·cm at decreasing porosity and interpartial fracture mechanism at 1300 – 1400°C; it becomes almost zero at mixed fracture mechanisms containing cleavage (1450 – 1500°C), and increases to 13 Ω·cm during the recrystallizing grain growth.

Concerning the final dependence of the strength of 1Ce10ScSZ electrolyte *σ* on its structure, and sintering temperature, it might be described as follows:

$$\sigma\,(T_s) = \left(\sigma_0 + K_\gamma(T_s)/\sqrt{d(T_s)}\right)\cdot(1 - P(T_s))^n$$

where σ_o is a structural part of the strength of some non-structural nonporous material, and equals 104 MPa; K_γ – coefficient dependant on quality of grain boundaries, and fracture micro mechanism; *d* – grain size; *P* – porosity, and T_s – sintering temperature [16].

The Structure and Properties of EB-PVD Film

EB-PVD is a promising process that might enhance the electrochemical performance of CFC. EB-PVD deposited layers contribute to the CFC lifetime increase and their cost reduction. CFC based on 1Ce10ScSZ electrolyte deposited by EB-PVD has demonstrated an area specific resistance of ~0.6ohm·cm² at 600 °C and a He leakage rate below 10^{-4} mbar·l·cm^{-2}·s^{-1} [8]. The conductivity of EB-PVD deposited films on a NiO-8YSZ anode is ~50% higher than that of layers made with traditional SOFC technology [9]. The

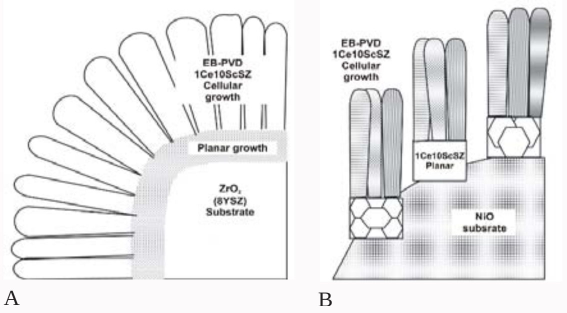

Figure 5: The schemes of the EB-PVD 1Ce10ScSZ structures observed on the 8YSZ (A) and the NiO (B) substrates [9].

data were obtained from the first attempt, with no any optimization.

This high performance is the result of a joint contribution of 1Ce10ScSZ powder, ensuring high electrolyte conductivity, and the electron beam technique, ensuring dense unidirectional nano-sized structure on highly porous NiO-8YSZ anode substrate. Additionally, a strong adhesion of the EB-PVD electrolyte to the porous anode is achieved, which is a very important prerequisite for any SOFC as an electrical device where quality of electrical contacts is vitally important.

The data obtained with transmission and scanning electron microscopy of the transitional zone between an EB-PVD zirconia film and its porous NiO-ZrO_2 substrate (AEI, anode – electrolyte interface) have allowed formulating plausible mechanisms of the ZrO_2 condensation from its vapor phase on ZrO_2 and NiO substrates during the EB-PVD process [9]:

The ZrO_2 condensation occurs in two stages with two mechanisms of growth – planar and cellular – by analogy with the solidification of the liquid as it is represented schematically in Figure 5. Furthermore, the condensation of ZrO_2 on NiO and ZrO_2 phases of the NiO-ZrO_2 composite occurs with two different routes.

Condensing on the ZrO_2 phase at the planar growth stage, the ZrO_2 film is covering the ZrO_2 grain surface entirely by a continuous layer of ~0.3-0.5 μm thickness that is followed by dense long cells/filaments resulting from cellular growth. The layer of planar growth is very defective and probably amorphous. After annealing, it becomes nanoporous. The planar ZrO_2 film on ZrO_2 substrate might be termed as nucleated with the "defective layer by defective layer" mechanism. The cells / filaments nucleate on the planar layer with no visible orientational preference.

Condensing on the NiO phase at the planar growth stage, the ZrO_2 film is discontinuous and porous. It consists of isolated "islands" / cells separated by rather big gaps / flaws, tough the "islands" themselves have no visible density defects even after annealing. Having reached about 0.5 to 0.7 μm of length, the "islands" change their growth mechanism from planar to cellular one and secondary cells / filaments are nucleated like branches of a bush. The "islands" may be either monocrystalline or polycrystalline, but they are dense. It indicates that the "islands" could be formed with a "dense layer by dense layer" mechanism. But in contrast to the ZrO_2 – ZrO_2 nucleation, the initial ZrO_2 cells nucleated on NiO grow with well-visible orientational preference, probably [100], as if they are growing into the NiO substrating grain.

The original transmission electron microscopy picture of AEI related to NiO phase is shown in Figure 6.

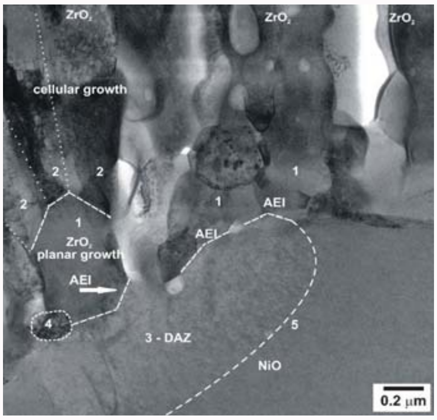

Figure 6: Schematic reconstruction of ZrO_2 bush nucleation and growth on a NiO grain. The ZrO_2 bush consists of a short trunk (1) grown during planar growth and followed by a few branches (2) grown with the cellular mechanism as laminated cells/filaments. The laminarity results from the constitutional supercooling and technical instabilities occurring during their growth. The bush is sited on its deposition affected zone (3) of the NiO substrate and is separated from it by the hardly visible anode-electrolyte interface. 4 is the NiO twin. 5 is an imaginary boundary of the deposition affected zone stripe in the NiO substrate grain [9].

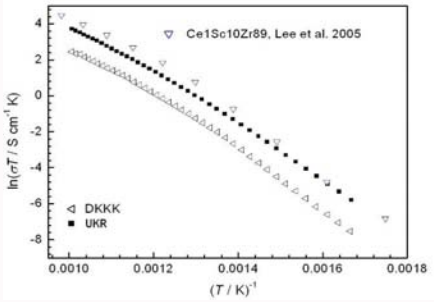

Figure 7: The total conductivity (bulk and grain boundary) vs. temperature for the 1Ce10ScSZ electrolytes: ■ – Ukr, Δ – DKKK.

The deposition affected zone surrounding the nucleation site of ZrO_2 on the NiO substrate is clearly discerned. It is a result of the entire phenomenon complex related to interaction of atoms and their clusters with a substrate in a full analogy with the heat affected zone well-known in welding of metals.

The structural features related to the ZrO_2 root at the ZrO_2 – NiO interface may be responsible also for the high adhesion of zirconia films deposited on porous NiO– ZrO_2 composites with EB-PVD.

High density of the planar growth layers and the existence of the deposition affected zone as well as doping it with Ni are probably responsible for the increased elasticity modulus of the film areas bordering the anode-electrolyte interface [7].

Lateral growth of secondary branches / filaments and orientational independence of zirconia-on-zirconia growth are the reasons of good coverage of highly porous NiO–ZrO_2 composites by the dense zirconia film meeting SOFC requirement for He leakage.

The Conductivity of Bulk and Film 1Ce10ScSZ Electrolyte

Figure 7 presents the Arrhenius plot of total electrical conductivity of bulk samples, measured via a.c. impedance at the temperature

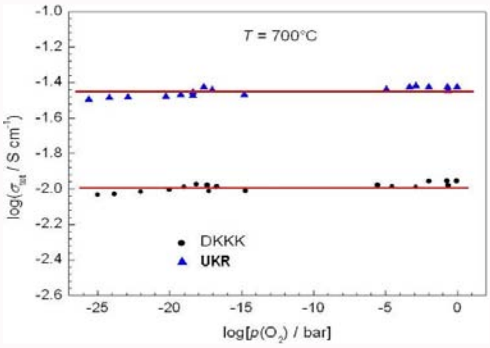

Figure 8: The total conductivity (bulk + grain boundary) of the 1Ce10ScSZ electrolytes as a function of partial pressure of oxygen, p(O_2), at 700 °C: ▲ –Ukr, ● – DKKK.

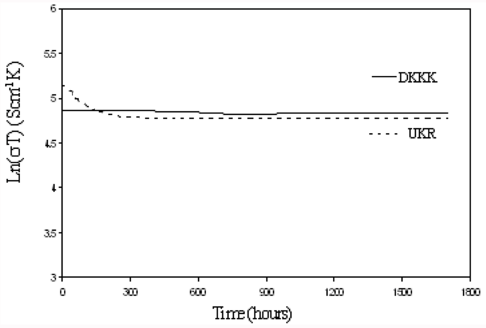

Figure 9: Long-term conductivity of electrolyte made of our and commercial 1Ce10ScSZ powders in air at 800 °C (---Ukr and —DKKK).

ranges of 350–727 °C in air [3]. The maximum conductivity value in this range is 0.036S·cm^{-1} at 727°C. The total electrical conductivity of our sample is higher than the one measured for the commercial DKKK ceramic samples on the whole range of temperatures. At higher temperatures, the conductivity values for our material overpasses DKKK one. The activation energy is 1.02eV up to 727°C, decreasing to 0.73eV above this temperature. The total conductivity (bulk and grain boundary) at 700°C as a function of partial pressure of oxygen log p(O_2) is represented in Fig. 8 also showing that the conductivity of IPMS electrolyte is higher than DKKK one. It is possible to assume that the overall conductivity could be increased further by improving the sintering properties of Ukrainian powder.

Figure 9 depicts the long-term testing in air, for 1500 hours at 800°C, showing an initial decrease in conductivity for our sample of about 25% within 300 hours followed by a constant evolution in time; in contrast, the conductivity of the commercial DKKK sample is almost constant for the time measured. Even like that, after 300 hours the conductivities of the two samples are almost similar. The probable reason of such the behavior of conductivity with temperature is the difference in both the size of initial particles of powders and their ability to recrystallization taking place during testing.

Thus, at short-term testing, the electrical conductivity measurements at 250-800°C indicated that the 1Ce10ScSZ-Ukr conductivity of bulk samples is higher than the conductivity of the commercially available samples for around one order of magnitude.

On long-term testing, although our sample exhibits a continuous decrease of the conductivity value in the first 300 hours, the attained value remains constant for the rest of the period and is almost displayed by the commercial sample. These conductivity values could be further improved by optimizing the sintering conditions for Ukranian powder that already demonstrated a promising alternative to the commercial electrolyte materials.

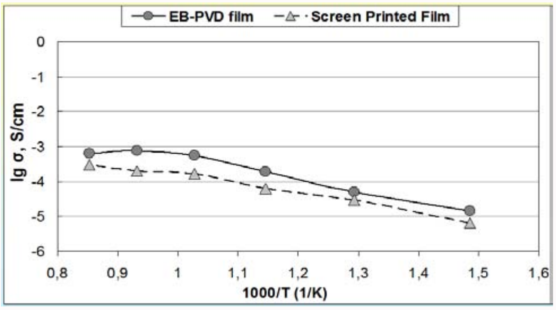

Figure 10: The total conductivity of nano-sized 1Ce10ScSZ electrolyte films deposited on Ni-8YSZ anodes with EB-PVD and screen-printing techniques [7].

As to EB-PVD 1Ce10ScSZ film, its electric conductivity was measured with specially designed samples in order to measure conductivity along the film thickness just as oxygen ions move in the electrolyte of real cell.

EB-PVD electrolyte film was deposited on reduced Ni-8YSZ anode. The conductivity was measured in the temperature interval 400–900°C and compared with conductivity of screen-printed film deposited on the same anode. The detailed information might be found in [7].

Figure 10 clearly shows that conductivity of EB-PVD electrolyte film is higher for around 50 % than that of the layer deposited by screen-printing usually used for electrolyte deposition at current CFC production.

The difference found in the behavior of electric conductivity of compared films is probably results from the principal difference in their structures. The structure produced by EB-PVD, as it was seen above, is practically as right columnar one. Such the structure may ensure the shortest ways for oxygen ions – carriers of electric charges. Commonly used screen-printed or tape-casted films have principally another structure. They are polygonal where ions should move along some longer zigzag ways.

The Catalitic Activity of Zirconia Powders

SOFC utilizes a gaseous fuel (hydrogen, methane etc.), which are oxidizing under the reaction of methane deep oxidation with oxygen as follows, e.g.:

$CH_4 + 2O_2 = CO_2 + 2H_2O$,

Forming water H_2O and carbon dioxide CO_2, which may subsequently react with methane under operating conditions of the fuel cell (temperature is 600-800°C, catalyst is Ni). Besides that, there can be the reaction of methane partial oxidation.

Except temperature, reactions between fuel gases and oxygen are needed in catalyst. Fortunately, all the constituents of CFC anode electrode, electronic and ionic conductors, Ni and ZrO_2, are good catalysts.

The fullest representative of the CFC process is heterogeneous-catalytic oxy-dry-steam reforming of methane, i.e. combination of reactions of conversion and oxidation of methane. Water, which is

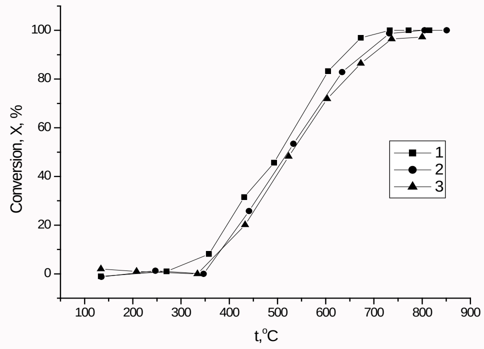

Figure 11: Dependencies of methane conversion on temperature with samples of Ni-10Sc1CeSZ anode at different nickel contents: 1) – 10%, 2) – 20%, 3) – 40%.

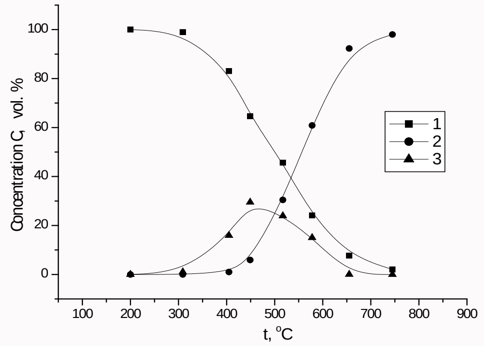

Figure 12: Concentration dependencies of methane, carbon monoxide, and carbon dioxide on temperature with samples of the 20Ni - 1Ce10ScSZ catalyst. 1) - CH_4, 2) - CO, 3) - CO_2.

formed in the process of methane oxidation, results in decreasing a negative coke deposits on surfaces of the catalyst.

Catalytic properties of samples of model Ni–ZrO_2 anodes in reaction of the steam conversion of methane were studied [20]. Catalytic activity of Ni – catalyst based on 12YSZ, 8ScSZ, and 1Ce10ScSZ carriers was characterized by conversion of CH_4 into CO_2 and temperature of achievement of 10%, 50%, and 90% levels of the methane conversion. Initial gases and products of reactions (CH_4, O_2, CO_2, CO) were analyzed chromatographically.

The dependence of methane conversion with Ni–10Sc1CeSZ catalysts at different Ni content, namely 10, 20, and 40% reduced preliminary in hydrogen, on temperature is shown in Figure 11. It is obvious that during methane steam conversion the catalyst with 20% Ni is more active than catalyst with 10% Ni. Its 10%, 50%, and 90% methane conversion are achieved at 40-45°C temperature below than it is possible to achieve with 10% Ni catalyst whereas activity of 20% Ni and 40% Ni samples are practically the same.

The temperature dependences of concentration changes of methane and products of conversion CO and CO_2 are shown in Fig. 12. We see that in the beginning of the process at temperatures 250-450 °C methane converts into CO_2 mainly with 20 % Ni – 10Sc1CeSZ catalyst. The maximum of conversion into CO_2 is observed at 400-450 °C. At temperatures above 700°C, methane converts mainly into CO where its selectivity reaches ~100 %.

The dependences of methane conversion on temperature with 20% Ni catalyst based on 12YSZ (1), 8ScSZ (2), and 1Ce10ScSZ (3) carriers preliminary reduced in hydrogen are shown in Figure 13. It is seen that catalysts based on 8ScSZ and 1Ce10ScSZ powders have practically equal activities in the reaction of steam conversion of methane. The catalyst based on 12YSZ powder has better activity namely its 10%, 50%, and 90% conversion of methane are achieved at lower for 20-25°C temperatures than with 8ScSZ and 1Ce10ScSZ powders. At temperatures above 730°C, all the catalytic samples have practically the same activity; the conversion of methane consists of 98-99%.

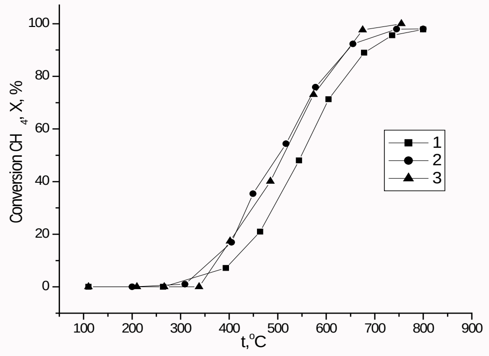

Figure 13: Dependencies of methane conversion on temperature tested with 20 % Ni catalyst based on carriers: 1) 12YSZ, 2) 8ScSZ, 3) 1Ce10ScSZ.

Thus, Ni–ZrO_2 composites based on Y- and Sc-stabilized cubic zirconia have revealed different activity in the reactions of deep oxidation and steam reforming of methane. Varying content of such systems enables regulation of the amount and mobility of oxygen in them and optimize the redox properties of the catalysts. The cataltic activity of YSZ based Ni–ZrO_2 composite is higher than ScSZ based one.

The Reduction of Nickel

The anode electrode operates principally in a reducing atmosphere induced by the fuel, but oxygen may occasionally occur in its compartments caused by diffusion from the cathode side or imperfect gas seals in the system. The typical material used for a CFC anode is a ceramic-metallic composite (cermet) made of yttria, or scandia stabilized zirconia (YSZ or ScSZ) and nickel. Metallic nickel is produced during the first hours of the operation of a CFC when a NiO phase is exposed to the fuel, which acts as a reducing agent. This reduction is accompanied by reduction in volume, which creates additional pores and cracks that improves the gas permeability of the anode but worthens its mechanical strength.

It is frased usually that the suggested degradation mechanisms are related mostly to the coarsening of Ni particles and the decrease of density of the three phases (Ni–ZrO_2–pore) boundaries. The volume changes attributed to reduction and oxidation influence strongly the integrity of the phase interfaces and their length.

Detailed study of structural changes in NiO–ZrO_2 composites with scanning and scanning transmission electron microscopy of porous NiO–10Sc1CeSZ anode composites in the initial state and after reduction in dry pure H_2 and model fuel gas–5-vol. % hydrogen with 95-vol. % Ar at 600°C for 4 hours shows as follows [21]:

In the initial material, the NiO phase exhibited facetted cubic and hexagonal shapes. The zirconia phase appeared smooth and as-fused with no signs of faceting. The boundaries between the two composite phases were smooth indicating a strong connection between them.

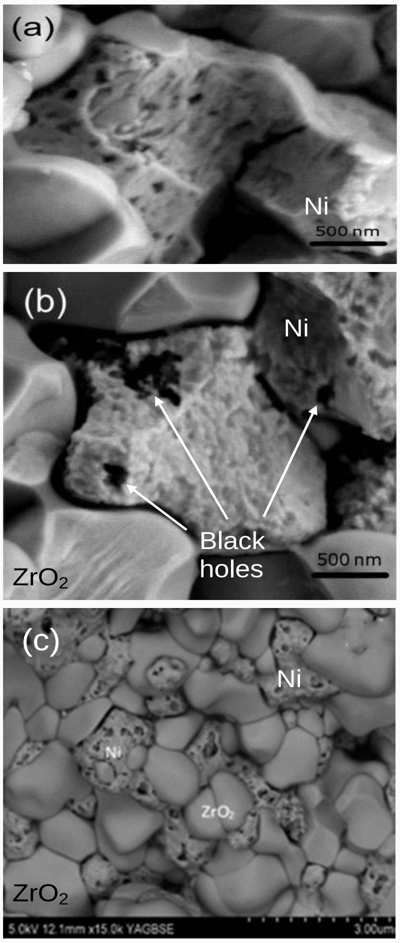

Figure 14: SEM images of surfaces of the reduced Ni-phase grains. (a) Reduced in 5-vol. % H_2 – Ar, (b) in H_2, both at 600°C for 4 hours, and (c) in H_2 at 800°C for 2 hours.

Reduction in dry pure H_2 resulted in the transformation of the NiO phase into a metallic Ni sponge with cracking along the Ni–ZrO_2 interfaces and a dramatic decrease in the mechanical strength.

In samples reduced in a mixture of 5-% H_2–Ar mixture, a porous Ni phase structure was not evident, particularly for grains of size greater than 1µm. In this case, the anode Ni phase consisted of a nanocrystalline Ni shell and a NiO core. Detailed investigations of Ni and Ni-NiO interface area have shown the presence of nanosized precipitates (~15nm) enriched with scandium and oxygen. They are suspected of being the result of inter diffusion promoted by H_2 at 600°C.

As to mechanisms of the hydrogen reduction and coarsening of the Ni-phase, it is seen that they might be determined as the hydrogen corrosion, which is like corrosion of metallic materials. The fractographic data evidences with no any doubts that during H_2 reduction the surface of the NiO-phase is changed with the pitting looking as nano-sized dimples while ZrO_2-phase does not subject any visible changes and remains as smooth and flat (Figure 14). The NiO-phase transforms into the Ni-sponge of larger size that at small magnifications of light microscopy of polished cross-sections looks as coarsening of Ni particles. Furthermore, the surface of Ni-grains contains some "black" areas typical for hydrogen corrosion of steels (Figure 14b). The feature evidences that these parts of Ni-boundaries are holes, entrances into a body of Ni-grain, which cannot give secondary electrons in order to build SEM image because they are empty, they are holes.

As to the electronic conductivity of reduced Ni–ZrO_2 composite λ_{cM}, it may be determined as

$$\lambda_{cM} = \lambda_1 \cdot (1 - 1{,}2 \cdot \theta_3),$$

where λ_1 is the specific conductivity of Ni, θ_3 is the partial volume of ZrO_2 phase [22].

The Redox of Ni–ZrO_2 Composites

Redox (reduction–oxydation) procedure proved to be useful. Studing the influence of structural transformations in the nickel phase during the redox cycling at 600°C temperature on strength and electric conductivity of NiO-ZrO_2 composites, significant improvement and stabilization of structure (Figure 15) and properties were obtained [23,24].

The Structural Optimization of CFC

It is possible to observe that during production, with both conventional and perspective techniques, and operation, CFC materials undergo degradation processes while under the combined influence of temperature, gas environment, contacts with inner and outer neighbors, electric current, mechanical stress, time etc. Traditionally, these processes are considered as negative and undesirable because they cause very serious structural alterations, chemical, which are related to local redistribution of chemical composition, and morphological, that not may not affect on their properties. At this, the effect is negative, and finally the CFC will degrade during operation.

The task is to prevent the drastic decrease of properties. We propose to transform the degradation processes into the useful instrument of positive changes, which will result in improvement of necessary properties of materials. By other words, we propose to optimize the structure of the CFC as a whole using the processes, which are responsible for negative effects in virgin CFC materials, in order to create the perfect CFC, structure and properties of which will be unaltered for a long time of operation. Speaking more expressively, we propose to use degradational negative processes for the sake of positive changes as some "positive degradation" in order to adjust the virgin materials and, thereby, provide the fuel cell by the stable optimal structure [25].

Such the replacement of the degradation from its negative to positive sense might be considered as an overall concept underpinning the structural optimization of CFC, which may have initially low or high but unstable properties, into devices of the stable structure, phase, geometrical and chemical, ensuring high performances. This "positive degradation" will make CFC of a high possible performance for operation during dozens of years at minimal maintenance.

As to the road-map how the structurally optimized SOFC could be achieved, it is necessary to know, which the approach of a suitable, optimized, structure might be accepted, the knowledge of degradation processes occurring in CFCs during their production and operation must be understood well. This knowledge would be gained from virgin materials, and as-produced and as-operated CFCs by means of traditional for materials science the comparative study and comprehensive structural characterization with various techniques such as electron microscopy and related techniques, x-ray phase analysis, nuclear magnetic and electron spin resonance

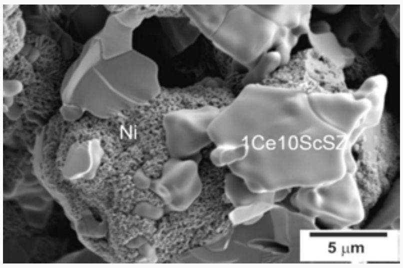

Figure 15: SEM picture of CFC fracture cross-section demonstrating well-suited to each other 1Ce10ScSZ electrolyte and Ni conductor of the CFC anode processed with a low-cycle redox training.

spectroscopies, impedance spectroscopy of electrical resistivity etc. Because CFC is a laminar composite, the knowledge of its structural and chemical heterogeneity at initial and post-operational states and the comparison of both of them is essential for understanding the phenomena of degradation and using it with the goal of implementation of CFC long-term operation at high performance.

Also, the characterization of mechanical and electrical behaviors of CFC at material and system levels in different environments, temperatures, mechanical loadings, and various redox and mechanical cycling is necessary. This knowledge would be obtained by long-term testing of fuel cells under realistic conditions with hydrogen, natural gas or bio-fuels at different temperatures and loadings in order to determine which fuel cell or technological process is more suitable for application and/or prescribed fuel. Because the CFC is a device of very long-term operation and the research-pioneers are not able to wait the final result, the CFC degradation must be modelled appropriately in order to predict the behavior of the fuel cell system.

For the electrolyte, as the first reference point for subsequent comparison, the zirconia powders of conventional composition, e.g., 1Ce10ScSZ, which are developed specially for electrolyte and electrodes, would be suitable. CFCs made of these virgin materials would be tested in order to obtain the reference data that jointly with data on structural and chemical heterogeneity, mechanical and electrochemical behaviors will be defined as the first reference point for the further iteration actions. Using these data and data already available including the literature ones, the parameters of zirconia powders will be refined for the second step of experiments, which will be repeated to optimize powders, their fine chemical composition and morphological features and the entire CFC, via a few iteration steps. Three of them, we are hoping, would be enough to obtain the optimized CFC structure.

The chemical composition of powders will be optimized using iterative processes of substance transfer from initial virgin, powders into the electrolyte layer of the CFC laminated composite, which is changed by diffusion processes between CFC electrolyte and its electrode layers during CFC production and its long-term operation. i.e. the final, corrected and optimized chemical composition of electrolyte layer and zirconia constituent in electrodes will be tuned by taking into account changes that occurs during both production and operation of the CFC in order to obtain the longevity in the final product – the fuel cell system operating at 600°C or below.

Decrease in the operating temperature to, e.g., 600°C, could positively impact on lifetime and costs of CFC systems, thereby facilitating the commercial introduction of clean and efficient CFC technology for heat and power generation.

Thus, the structural optimization is targeted for the radical improvement of ionic conductivity of the critical CFC cell component – the oxygen ionic conductor of electrolyte and electrodes – by using optimized 10Sc1CeSZ zirconia powders tuned for long-term high ionic conductivity and stability in real materials, gas environments and electrical loads. The aim is to improve the ionic conductivity by a factor of minimum three in comparison with available materials on the world market.

It is understandable that the goals might be achieved by joint simultaneous highly qualified efforts in different disciplines including materials science first of all, chemistry, electrochemistry, thin films, mechanical behavior, catalysis and computer modelling. The working Programme must include as follows: zirconia powder synthesis and sintering, thin film deposition with tape casting, and electron beam and magnetron sputtering deposition, comprehensive materials characterization with electron beam and related techniques, x-ray, and nuclear magnetic and electron spin resonance techniques, mechanical and electrochemical behaviors at different mechanical and electric loads in different atmospheres and over time, impedance spectroscopy in a wide temperature interval, modelling and prediction. All the listed is very expensive research activity affordable mainly for the USA or whole the European Union.

The main achievements, which led the authors to understanding that the ambitious intention of the CFC structural optimization would be realized are as follows:

The ionic conductivity of bulk and film electrolytes made of Ukrainian (Ukr, Type I) 1Ce10ScSZ powders is $0.035 S \cdot cm^{-1}$ at 700°C instead of the $0.010 S \cdot cm^{-1}$ obtained with the best powders traditionally used at international scale. An electrolyte made of Ukrainian powder has the highest strength (450MPa), fracture toughness – $1.2\text{-}1.7\ MPa \cdot m^{1/2}$, and so on. This electrolyte is much less inclined to recrystallization.

The ionic conductivity of EB-PVD electrolyte films deposited onto a porous $NiO\text{-}ZrO_2$ anode substrate is much higher (half an order of magnitude) than of conventional layers deposited, e.g., by screen printing.

CFC made with EB-PVD electrolytes were the first to pass the severe Juelich Research Center, Germany, standard for He leakage $9.3 \cdot 10^{-05}$ $mbar \cdot l/(sec \cdot cm^2)$.

The processing of $NiO\text{-}ZrO_2$ anode composites with low redox cycling results in significant improvement of the electrical conductivity and mechanical strength of the $Ni\text{-}ZrO_2$ anode cermet.

The structural optimization might be easily realized, if all the steps of a long CFC creation process could be united under one research project acting under the "from powder to power" concept, i.e., it begins from powder synthesis and completes by CFC testing via comprehensive structural characterization of powders and their transfer into CFCs, behavior characterization of their electrical and mechanical properties in different gas environment and at different mechanical and electrical loadings, catalytic activity both electrodes and their new concepts, integration into technically relevant cells and stacks, and long-term tests.

Finally, at the last stage of the study, the stage of the "positive degradation", using data obtained for powders and CFC, materials will be modified and optimized in order to get a positive effect on the CFCs long-term performance at their usage in energy systems. The

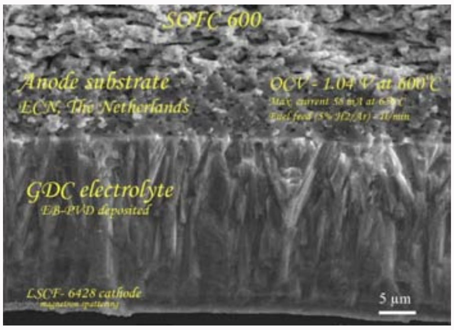

Figure 16: SEM picture of fracture cross-section of CFC made with EB-PVD technique.

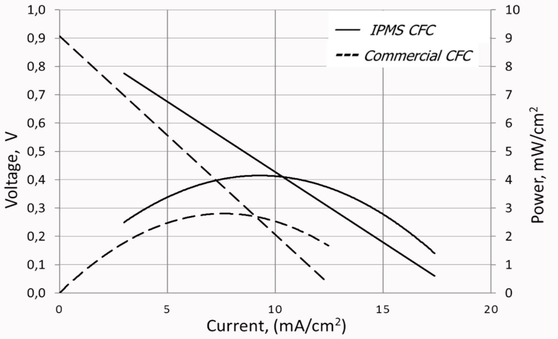

Figure 17: The comparison of electrochemical properties of newly developed 8YSZ CFC and its commercial analog fueled with model fuel 5-vol. % H_2 in Ar, and tested with Medusa RD 100 series 890CL fuel cell test station, Scribner, USA, at 800°C.

CFC, which has no any delaminating cracks along contacts between its structural parts that is very important for any electro technical device, might be elaborated (Figure 16).

The CFC`s technology is rather mature already and they might be put into commercial production now. Nevertheless, the opportunities (for development) are endless. 3D printing is imminent.

Transiting to Mass-Production

Ukrainian CFC team has legalized their activity thanks the small IPMS search project under the title "Ceramic fuel cells based on zirconia stabilized with scandium and (Sc–Y) systems", in 2000, when the first Ukrainian ceramic fuel cell was demonstrated. Slowly but steadily, the study has developed as research of CFC materials mainly. The first samples of CFCs were produced with traditional powder techniques based uniaxial pressing of own zirconia powders and their sintering, and later with EB-PVD deposition of zirconia electrolyte.

Now, Laboratory for CFC founded in 2015 at IPMS is developing the pilot technology for production of CFC using tape-casting technique usually used for such purposes. Figure 17 demonstrates the first data on the test of new CFC compared with CFC available at the world market. CFC was tested with the model fuel gas, 5-vol. % H_2 in Ar, at 800°C.

It is seen obvious better result of Ukrainian CFC that is based on better properties of 8YSZ zirconia powders specially developed for CFC electrolytes. Being fueled with pure hydrogen, new CFC based on 8YSZ electrolyte could ensure 4.2kW/m² at temperature 800°C.

Conclusions

Ceramic Fuel Cells in Ukraine have overcome a complicated long way of research and development since 1993 from zirconia powders to the first in Ukraine working samples of namely ceramic fuel cells demonstrating promising properties and able to operate at 600°C. CFC R&D are developing in Ukraine as "materials science for ceramic fuel cells" based on a study of thin, nano-sized, structure and its influence on properties of both separate CFC materials and whole the CFC, and where electrochemistry and its impedance spectroscopy are intrinsically involved in the study of thin structure, especially in those cases where traditional thin structural methods are not able to answer on very important questions on the role of interfaces like grain or subgrain boundaries in formation of whole complex of material properties.

Acknowledgements

We are grateful to the National Academy of Science of Ukraine, their projects "Structural Fundamentals of Materials for Zirconia Ceramic Fuel Cells" and "SOFC structural optimization based on consideration of interdiffusion at manufacturing and operation", and current ones; NATO, their "Science for Peace" project №980878 "Solid Oxide Fuel Cells for Energy Security", the European FP6 projects: №SES6-2006-020089 "Demonstration of SOFC stack technology for operation at 600°C (SOFC600)" and students exchange program of the "Real SOFC", INTAS project "Structure Optimization of SOFC Based on Scandia Doped Zirconia Ceramics for Space Application", FP7 project "Deployment of Societally Beneficial Nano- and Material Technologies in European Partnership Countries" (FP7-NMP-2013-CSA-7) for their respective supports.

We are especially thankful our colleagues Prof. O. Ostash, Dr. O. Koval, Dr. A. Samelyuk, Dr. A. Kotko, Dr. M. Beha, Dr. B. Vasyliv, Dr. A. Ivasyshyn, Dr. V. Podhurska, Mrs. M. Holovkova, Dr. I. Brodnikovska, and Dr. D. Brodnikovsky, Prof. J. Irvine, Prof. A. Smirnova, Prof. R. Steinberger-Wilckens, Prof. J. Kilner, Dr. C. Savaniyu, Dr. M. Andrzeichuk, Dr. J. Grzhonka, Prof. M. Levandowska and Prof. Kurzydlowski. for their enthusiastic activity and support of obtaining new knowledge on ceramic fuel cell materials and their processing.

References

1. Föger K. From Powder to Power. Unpublished presentation at 11th International Symposium on Solid Oxide Fuel Cells (SOFC-XI). 2009; 11.
2. Akimov G, Vasylyev O and Koval O. Zirconia Ceramics and Their Prospects in Ukraine. Refractories and Technical Ceramics. 2000; 10: 2-5, in Russian.
3. Vasylyev O, Smirnova A, Brychevskyi M, Brodnikovskyi I, Firstov S, Vereshchak V, et al. Structural, Mechanical and Electrochemical Properties of Ceria Doped Scandia Stabilized Zirconia. Material Science of Nanostructures. 2011; 1: 70-80.
4. Grzonka J, Vereshchak V, Shevchenko O, Vasylyev O, and Kurzydlowski K. Characterization of Sc_2O_3&CeO_2-Stabilized ZrO_2 Powders via Co-Precipitation or Hydrothermal Synthesis. Microscopy and Microanalysis. 2013; 19: 29-32.
5. Lee DS, Kim WS, Choi SH, Kim J, Lee HW, Lee JH. Characterization of ZrO_2 Co-Doped with Sc_2O_3 and CeO_2 Electrolyte for the Application of Intermediate Temperature SOFCs. Solid State Ionics. 2005; 176: 33–39.
6. Haering C, Roosen A, Schichl H, Schnfller M. Degradation of the Electrical Conductivity in Stabilized Zirconia System. Part II: Scandia-Stabilized Zirconia. Solid State Ionics. 2005; 176: 261–268.

7. Vasylyev O, Smirnova A, Brychevskyi M, Pryshchepa Ie, Dubykivskyi L, Samelyuk A, et al. Zirconia EB-PVD Electrolyte Films: Structure, Mechanical Properties, and Conductivity. ECS Transactions. 2009; 25: 1687-1699.

8. Andrzejczuk M, Vasylyev O, Brychevskyi M, Smirnova A, Lewandowska M, Kurzydłowski K, et al. Structural Features and Gas Tightness of EB-PVD 1Ce10ScSZ Electrolyte Films, Matereials Science-Poland. 2012; 30: 170-179.

9. Vasylyev O, Brychevskyi M, Brodnikovskyi I, Firstov S, Andrzejczuk M, Spychalski M, et al. Nucleation and Growth Mechanisms of Zirconia Film Deposited on Porous Nickel Oxide – Zirconia Substrate by Electron Beam – Physical Vapor Deposition. Advances in Ceramic Science and Engineering. 2014; 3: 25-35.

10. Linderoth S, Bonanos N, Jensen K, and Bilde-Sorensen J. Effect of NiO-to-Ni Transformation on Conductivity and Structure of Yttria-Stabilized ZrO_2. Journal of the American Ceramic Society. 2001; 84; 11: 2652–2656.

11. Herle JV, Vasquez R. Conductivity of Mn and Ni-Doped Stabilized Zirconia Electrolyte. Journal of the European Ceramic Society. 2004; 24: 1177–1180.

12. White J, Reimanis I. The Enhanced Stabilization of the Cubic Phase in Yttria-Stabilized Zirconia with the Addition of Nickel Oxide. J Am Ceram Soc. 2011; 94: 2030–2036.

13. Vasylyev O, Brodnikovskyi I, Brychevskyi M, and Pryshchepa I. NiO-10Sc1CeSZ Anode: Structure and Mechanical Behavior. In: Advances in Solid Oxide Fuel Cells III: Ceramic Engineering and Science Proceedings. Ed. Narottam P. Bansal. Wiley. 2007; 28: 361-367.

14. Ostash O, Vasyliv B, Podhurska V, Vasylyev O, Brodnikovskyi Ye, Ushkalov L. The Optimization of 10Sc1CeSZ–NiO Composite with Redox Properties. Physics and Chemistry of Material Mechanics. 2010; 5: 76-81, in Ukrainian.

15. Brodnikovskyi Ye. The Regularities of Structure Formation, Mechanical Behavior, and Electrochemical Properties of Ni-ZrO2 Anode for Solid Oxide Fuel Cell. PhD Dissertation. IPMS, Kyiv. 2012; 21, in Ukrainian.

16. Brychevskyi M, Vasylyev O, Brodnikovskyi Ye, Firstov S, Samelyuk A. Effect of Sintering Temperature on Structure, and Mechanical Behavior of 1Ce10ScSZ Ceramics. Electron Microscopy and Strength of Materials. IPMS Annual Edition, Kyiv. 2013; 19: 169-183, in Ukrainian.

17. Chaim R. Activation Energy and Grain Growth in Nanocrystalline Y-TZP Ceramics. Materials, Science and Engineering. 2008; 486: 439-446.

18. Rice R. Microstructure Dependence of Mechanical Behavior of Ceramics. Treatise on Mater. Science and Technology. Ed. R. K. Mac Crone, Academic Press, NY. 1977; 11: 199-381.

19. Brodnikovska I, Brychevskyi M, Brodnikovsky Y, Brodnikovsky D, Vasylyev O, and Smirnova A. Joint Impedance Spectroscopy and Fractography Data Analysis of Ceria Doped Scandia Stabilized Zirconia Solid Electrolyte Modified by Powder Types and Sintering Temperature. To be published in French-Ukrainian Journal of Chemistry. 2018.

20. Shashkova T, Kantcerova M, Chedryk V, Vasylyev O, and Orlyk S. Methane Oxidation Conversion over the Composites of Y- and Sc-stabilized Zirconia Based. Polish J Chem. 2008; 82: 321-376.

21. Andrzejczuk M, Vasylyev O, Brodnikovskyi I, Podhurska V, Vasyliv B, Ostash O, et al. Microstructural Changes in NiO–ScSZ Composite Following Reduction Processes in Pure and Diluted Hydrogen. Materials Characterization. 2014; 87: 159–165.

22. Polishko I, Brodnikovskyi Y, Brodnikovskyi D, Vasyliv B, Podhurska V, Shevchenko S, et al. The Influence of Porosity on Mechanical Strength and Electrical Conductivity of NiO–3,5YSZ Composite and Its Ni–3,5YSZ Cermet. Powder Metallurgy. 2017; 5/6: 80-93.

23. Ostash O, Vasyliv B, Podhurska V, Vasyle O, Brodnikovskyi E and Ushkalov L. Optimization of the Properties of 10Sc1CeSZ–NiO Composite by the Redox Treatment. Materials Science. 2011; 46: 653–658.

24. Vasyliv B, Ostash O, Podhurska V and Vasylyev O. A Procedure of Treatment of NiO-Containing Anodes of Solid Oxide Fuel Cells. Patent of Ukraine. 2013; №78992, in Ukrainian.

25. Vasylyev O, Brychevskyi M, Brodnikovskyi Ye. The Structural Optimization of Ceramic Fuel Cells. Universal Journal of Chemistry. 2016; 4: 31–54.: